CORA Cork Open Research Archive
Cartlann Taighde Oscailte Chorcaí

Title	The evolution of resonance: a multiscale approach to the effect of nonlinearity, frequency dispersion and geometry
Authors	Mortell, Michael P.;Seymour, Brian R.
Publication date	2019-04-05
Original Citation	Mortell, M. P. and Seymour, B. R. (2019) 'The evolution of resonance: a multiscale approach to the effect of nonlinearity, frequency dispersion and geometry', Mathematical Modelling of Natural Phenomena, 14(4), 403 (20pp). doi: 10.1051/mmnp/2019005
Type of publication	Article (peer-reviewed)
Link to publisher's version	https://doi.org/10.1051/mmnp/2019005 - 10.1051/mmnp/2019005
Rights	© 2019, EDP Sciences. Copyright of Mathematical Modelling of Natural Phenomena is the property of EDP Sciences and its content may not be copied or emailed to multiple sites or posted to a listserv without the copyright holder's express written permission. However, users may print, download, or email articles for individual use.
Download date	2026-10-31 11:03:17
Item downloaded from	https://hdl.handle.net/10468/7823

UCC
University College Cork, Ireland
Coláiste na hOllscoile Corcaigh

Math. Model. Nat. Phenom. 14 (2019) 403
https://doi.org/10.1051/mmnp/2019005

Mathematical Modelling of Natural Phenomena
www.mmnp-journal.org

THE EVOLUTION OF RESONANCE: A MULTISCALE APPROACH TO THE EFFECT OF NONLINEARITY, FREQUENCY DISPERSION AND GEOMETRY

Michael P. Mortell[1] and Brian R. Seymour[2,*]

Abstract. Nonlinear resonant oscillations in continuous media contain two natural time scales: the travel time in the medium and the 'slow' time defined by the small nonlinearity. A multiscale approach is used to describe the evolution to a periodic state. We focus on three basic experiments that define nonlinear resonant oscillations in continuous media: a gas in both a straight tube and a tube of variable cross-section, and shallow water in a tank. The outcomes of these experiments are described and the mathematical techniques that show the evolution to the final periodic states are given in some detail.

Mathematics Subject Classification. 35L05, 35L67.

Received September 25, 2018. Accepted January 30, 2019.

1. Introduction

We deal with one-dimensional waves in a region of finite extent, so that reflections from boundaries are intrinsic to the problems considered and waves pass through each other. For linear theory solutions can be superposed and hyperbolic waves pass through each other without interaction or distortion. In contrast, the fundamental difficulty for nonlinear hyperbolic waves is that such waves interact and distort, see Riemann [31]. Then a wave travelling in one direction is affected by that travelling in the opposite direction and the characteristic equations cannot, in general, be integrated. There is, however, a class of nonlinear waves where, to first order in the amplitude, the waves do not interact while the signal distorts. Resonant oscillations in tubes and tanks belong to such a class.

Three basic experiments define nonlinear resonant oscillations in continuous media. Here, these experiments are described and then the associated mathematical solutions explained using multiscale techniques. All examples contain two natural time scales: the travel time in the medium and the 'slow' time defined by the small nonlinearity. The first experiment involves small amplitude resonant acoustic oscillations in a closed tube and the appearance of shocks in the flow. Saenger and Hudson [32] observed that the shocks travel with the linear sound speed and do not interact after reflection. The most comprehensive analysis of this phenomena was first given by Chester [4]; we will use a "nonlinearization" approach to arrive at the same result, see [27, 28]. The second experiment involves resonant acoustic oscillations in a tube of varying cross-section, *e.g.* a cone or bulb shape, see [22]. Due to the interaction of nonlinearity and the geometry, the motion of the gas can have a

Keywords and phrases: Nonlinear wave, resonance, evolution.

[1] Department of Applied Mathematics, University College Cork, Cork, Ireland.
[2] Department of Mathematics, University of British Columbia, Vancouver, Canada.

* Corresponding author: seymour@math.ubc.ca

Article published by EDP Sciences

© EDP Sciences, 2019

large amplitude and yet remains continuous. The analysis is given in [26, 28]. The final experiment, reported on by Chester and Bones [6], concerns resonant sloshing of shallow water in a tank. The presence of frequency dispersion, which spreads the wave and counteracts the steepening due to nonlinearity, ensures the fluid motion is continuous. The outcome is a series of solitary waves whose number and height depend on the frequency and is governed by a periodically forced Korteweg–de Vries (KdV) equation, [12, 28].

In each case, the final analytic result shows that the motion is a linear standing wave, but with the signal carried by the waves determined at a higher order by a nonlinear equation. Specifically, the standing wave for the closed tube of constant cross-section, see [4, 32], and the resonant sloshing in a closed tank, [5, 12], is the superposition of oppositely travelling linear waves in which the signal carried is determined from a nonlinear p.d.e. In the case of the tube with variable cross-section [22, 26], the standing wave has an arbitrary amplitude and phase, as in linear theory, that are determined by coupled nonlinear o.d.e.s at higher order. The nonlinearization technique, [27, 28], is extended using a multiscale expansion to the analysis of the evolution to the periodic state and is seen to simplify the higher order calculations. The basic idea is that when the linear travel time is corrected, the nonlinear solution emerges, and the singularity in the acoustic solution is avoided. The context of this last sentence is as follows.

A straight gas-filled tube, closed at $x = 0$, has a vibrating piston at $x = 1$ with piston velocity $M\sin(2\pi\omega t)$. According to acoustic theory the velocity $u(x,t)$ of the gas satisfies the one-dimensional wave equation:

$$\frac{\partial^2 u}{\partial t^2} - \frac{\partial^2 u}{\partial x^2} = 0,$$

where the sound speed has been normalized to unity. Together with the boundary conditions, these lead to the difference equation for $g(t)$

$$g(t) - g(t-2) = M\sin(2\pi\omega t),$$

where

$$u(x,t) = g(t+x-1) - g(t-x-1).$$

Then

$$g(t) = -\frac{M}{2\sin(2\pi\omega)}\cos(2\pi\omega[t+1]), \quad \sin(2\pi\omega) \neq 0.$$

The condition $\sin(2\pi\omega) = 0$ implies $\omega = \omega_n = n/2$, $n = 1, 2, 3, \ldots$ that define the *resonant frequencies* ω_n where the acoustic solution has singularities. At the fundamental resonance, $\omega_1 = 1/2$, the period of the piston input is $T = 2$, which is also the travel time in the tube and hence also the difference in the difference equation. When the travel time and period coincide there is no periodic solution to the difference equation. The insight given here is that if we correct the travel time by including nonlinearity, the difficulty of the singularity in the acoustic solution is bypassed and a bounded nonlinear solution emerges.

This insight, which is a generalization of Whitham's nonlinearization technique [40], gives an observation into the essential physical understanding of the phenomena under investigation, and also simplifies the calculation of nonlinear terms. It is used to analyze experiments 1 and 3 in Sections 2 and 4.

The analysis of Section 3 requires a different technique and here the key experimental observations are the incommensurability of the resonant frequencies, *i.e.*, $\omega_n \neq n\omega_1$, the hysteresis effect and the hard or soft resonant response depending on the container shape, see Figure 6.

2. Experiment 1: Resonant oscillations in a straight closed tube

There have been many experiments describing resonance in a straight closed tube. Among them are those of Lettau [23], Gulyaev and Kuzentsov [17], Galiev *et al.* [15], Sturtevant [37] and Saenger and Hudson [32]. An early review is given in Ilgamov *et al.* [20]. Here, we focus on the experiments of Saenger and Hudson [32] in which the results give a clear guide to an underlying theory.

- In a tube of length (L) 42 inches, diameter 1.9 inches and piston amplitude of 1/8 inch, shocks are observed at the closed end when the piston operates at frequencies near the fundamental.
- Oppositely traveling shock waves at higher resonant frequencies pass through each other without interaction, *i.e.*, they obey the rule of linear superposition.
- The shocks have constant strength and travel at constant adiabatic sound speed.
- The amplitude of the flow at resonance is significantly greater than that of the input.

The corresponding theory for the periodic motion was principally developed by Betchov [3], Chu and Ying [10], Gorkov [16], Chester [4] and Seymour and Mortell [33]. The evolution of such oscillations is given in Cox and Mortell [11, 13] for small rates and in Seymour and Mortell [36] for finite rates.

We show here how the resonant oscillations evolve to a periodic state using the concept of *nonlinearization* to simplify the calculations, see [27].

2.1. Multiscale expansion

The equations of conservation of mass and momentum for a polytropic gas in Eulerian coordinates are:

$$\frac{\partial \rho}{\partial t} + \frac{\partial}{\partial x}(u\rho) = 0, \;\; \frac{\partial u}{\partial t} + u\frac{\partial u}{\partial x} + \rho^{-1}\frac{\partial p}{\partial x} = 0. \tag{2.1}$$

with

$$\frac{p}{p_0} = \left(\frac{\rho}{\rho_0}\right)^{\gamma}, \tag{2.2}$$

where $u(x,t)$ is the velocity, $\rho(x,t)$ the density, γ the adiabatic constant (1.2 for air) and the reference state is (p_0, ρ_0). The associated linear sound speed is given by $c_0 = \sqrt{\frac{\gamma p_0}{\rho_0}}$, where in general $c^2 = \frac{\mathrm{d}p}{\mathrm{d}\rho}$. The variables (u, p, ρ, c, x, t) are nondimensionalized with respect to $(c_0, \rho_0 c_0^2, \rho_0, c_0, L, Lc_0^{-1})$, where L is the length of the tube.

The Riemann invariant form of the dimensionless equations (2.1) is, see Whitham [40] equation (6.71),

$$u \pm \frac{2}{\gamma - 1}c = \text{const.}, \;\; \text{on} \;\; \frac{\mathrm{d}x}{\mathrm{d}t} = u \pm c. \tag{2.3}$$

For $|u| \ll 1$, we assume the multiscale expansions for $u(x,t)$ and $c(x,t)$ in the form

$$\begin{aligned} u(x,t) &= Mu_1(x,t;\tau) + M^2 u_2(x,t;\tau) + \dots \\ c(x,t) &= 1 + Mc_1(x,t;\tau) + M^2 c_2(x,t;\tau) + \dots, \end{aligned} \tag{2.4}$$

where the time scale $\tau = Mt$ allows for the slow evolution to the periodic state. $M \ll 1$ is the Mach number of the input. The boundary conditions are a closed end at $x = 0$ and an oscillating piston at $x = 1$:

$$u(0,t;\tau) = 0, \;\; u(1,t;\tau) = M\sin(2\pi\omega t). \tag{2.5}$$

The period of the piston is $1/\omega$ so that periodicity requires $u(x,t+1/\omega;\tau)=u(x,t;\tau)$. Periodicity together with (2.1) and (2.5) implies that u satisfies the zero mean condition $\int_0^{1/\omega}u(x,t;\tau)\mathrm{d}t=0$.

At $O(M)$

$$\left(\frac{\partial}{\partial t}+\frac{\partial}{\partial x}\right)\left(u_1+\frac{2}{\gamma-1}c_1\right)=0 \text{ and } \left(\frac{\partial}{\partial t}-\frac{\partial}{\partial x}\right)\left(u_1-\frac{2}{\gamma-1}c_1\right)=0, \tag{2.6}$$

which imply

$$u_1(x,t;\tau)=f(t-x;\tau)+g(t+x-1;\tau),\ c_1=\frac{\gamma-1}{2}[f(t-x;\tau)-g(t+x-1;\tau)]. \tag{2.7}$$

f and g are arbitrary functions, with $g(t+1/\omega;\tau)=g(t;\tau)$ and $\int_0^{1/\omega}g(t)\mathrm{d}t=0$.

The boundary condition at $x=0$ implies $f(t;\tau)=-g(t-1;\tau)$ so that

$$u_1(x,t;\tau)=g(t+x-1;\tau)-g(t-x-1;\tau),$$

and the condition at $x=1$ is

$$\begin{aligned}\sin(2\pi\omega t)&=g(t;\tau)-g(t-2;\tau-2M),\\&=g(t;\tau)-g(t-2;\tau)+2M\frac{\partial g}{\partial\tau}(t-2;\tau)+O(M^2).\end{aligned} \tag{2.8}$$

At resonance, when g has period 2 in t and $\omega=1/2$, then (2.8) becomes

$$2M\frac{\partial g}{\partial\tau}(t;\tau)=\sin(\pi t),$$

or

$$g(t;\tau)=\frac{1}{2}t\sin(\pi t), \tag{2.9}$$

since $\tau=Mt$. This is the usual initial linear growth of an acoustic wave at resonance, see Figure 3.

2.2. Nonlinearization and evolution

Equation (2.8) is a linear differential-difference equation where the linear travel time in the tube is given by the difference 2, and this is the first approximation. We will correct equation (2.8) by inserting a nonlinear travel time to replace the linear travel time. This is referred to as the *nonlinearization* of (2.8), and allows us to go directly to the final equation for g without the usual calculations at $O(M^2)$, for example as in Chester [4].

The Riemann invariant form (2.3) can be written, on using (2.6) and (2.7),

$$u_1+\frac{2}{\gamma-1}c_1=2f(\alpha;\tau) \text{ on } \frac{\mathrm{d}x}{\mathrm{d}t}|_\alpha=u+c, \tag{2.10}$$

$$u_1-\frac{2}{\gamma-1}c_1=2g(\beta;\tau) \text{ on } \frac{\mathrm{d}x}{\mathrm{d}t}|_\beta=u-c. \tag{2.11}$$

The second experimental result in [32] in Section 2 here implies that we can treat $f(\alpha;\tau)$ and $g(\beta;\tau)$ as *simple waves*, see [28] or [40], since there is no interaction between f and g. Then from (2.10) for an $\alpha-$ wave

(with $g = 0$)

$$u_1 = \frac{2}{\gamma - 1} c_1 = f(\alpha; \tau), \tag{2.12}$$

and the $\beta-$ wave carries the signal $c_1 = 0$, $u_1 = 0$, or $u = 0$, $c = 1$.

From (2.10) and (2.12)

$$\frac{\mathrm{d}x}{\mathrm{d}t}|_\alpha = 1 + \frac{\gamma + 1}{2} M f(\alpha; \tau) + O(M^2), \tag{2.13}$$

and

$$\frac{\mathrm{d}t}{\mathrm{d}x}|_\alpha = \frac{1}{u + c} = \frac{1}{1 + \frac{\gamma+1}{2} M f(\alpha; \tau)}, \tag{2.14}$$

which integrates to

$$\alpha = t - x + \frac{\gamma + 1}{2} M x f(\alpha; \tau) + O(M^2), \tag{2.15}$$

with $\alpha = t$ on $x = 0$. Similarly, for the $\beta-$ wave,

$$\beta = t + x - 1 + \frac{\gamma + 1}{2} M (x - 1) g(\beta; \tau) + O(M^2), \tag{2.16}$$

with $\beta = t$ on $x = 1$. These agree with the Lagrangian formulation as in Section 8.1.1 of Mortell and Seymour [28].

We note that from (2.10) and (2.11) that the signals u and c are calculated from *linear equations*, while the characteristics (2.15) and (2.16) involve *nonlinear* corrections. This is Whitham's nonlinearization technique, see [40], Chapter 9.

From (2.15), (2.16) and the boundary condition on $x = 0$, the *nonlinear* travel time, *i.e.*, the time to go from $x = 1$ at time t_0, reflecting off $x = 0$ where $u = 0$, and then returning to $x = 1$ at time t_2 is

$$t_2 - t_0 = 2 + (\gamma + 1) M g(t_0; \tau), \tag{2.17}$$

so that it now depends on the signal carried g.

Equation (2.8) becomes

$$\sin(2\pi\omega t) = g(t; \tau) - g(t - 2 - (\gamma + 1) M g(t; \tau)) + 2M \frac{\partial g}{\partial \tau}(t - 2; \tau) + O(M^2). \tag{2.18}$$

Exactly at the fundamental resonant frequency, when $\omega = 1/2$ and $g(t; \tau)$ has period 2 in t, we expand (2.18) for $|Mg| \ll 1$ to get

$$M \frac{\partial g}{\partial \tau} + \frac{\gamma + 1}{2} M g \frac{\partial g}{\partial t} = \frac{1}{2} \sin(\pi t). \tag{2.19}$$

This is the p.d.e. for the evolution of the motion at resonance. The linear term in (2.19) gives the initial growth, see equation (2.9), and as $\tau \to \infty$ the steady state equation with $\omega = 1/2$ is

$$\frac{\gamma + 1}{2} M^2 g(t) g'(t) = \frac{1}{2} M \sin(\pi t), \tag{2.20}$$

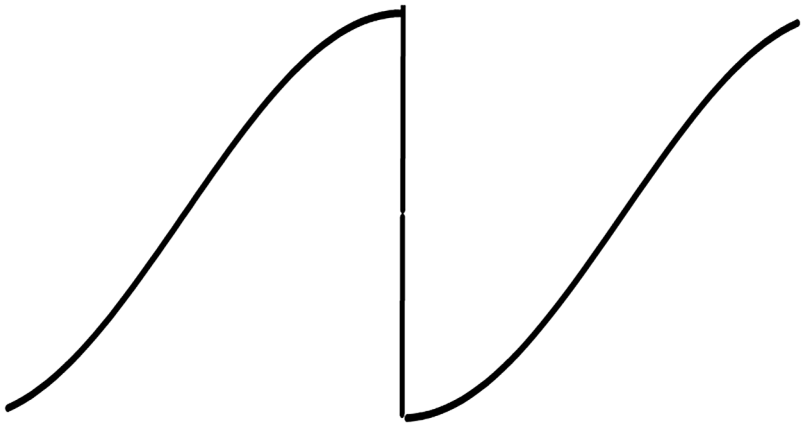


FIGURE 1. The two branches of the solution (2.21) joined with a shock.



FIGURE 2. Experimental pressure wave from [32].

which integrates to

$$Mg(t) = \pm\left(\frac{4M}{\pi(\gamma+1)}\right)^{1/2}\sin\left(\frac{\pi}{2}t\right),\ 0\le t\le 2, \tag{2.21}$$

with $g(t+2)=g(t)$. A shock is inserted at $t=1$ to satisfy the mean condition $\int_0^2 g(t)\mathrm{d}t=0$.

The steady state result at resonance is

$$u(x,t) = Mu_1(x,t) = M[f(t-x)+g(t+x-1)]+O(M^2),$$

where $f(t)=-g(t-1)$, so that

$$u(x,t) = M[g(t+x-1)-g(t-x-1)]+O(M^2), \tag{2.22}$$

where Mg is given by (2.21).

Thus $u(x,t)$, given by (2.22), is the superposition of linear waves travelling in opposite directions at the constant adiabatic sound speed. The waves do not interact and the signal carried is determined by a nonlinear o.d.e. with signal amplitude $|Mg|=O(M^{1/2})$. The zero mean condition implies there is a discontinuity between the two branches of the solution (2.21), which is a shock of constant strength in the signal g. This solution (shown in Fig. 1) matches the experimental results of Saenger and Hudson [32], see Figure 2.

If $\gamma = 2$ in (2.19) or (2.21), we have the result for nonlinear resonant sloshing in hydraulic flow in a shallow tank, see [39].

2.3. Detuning

We now consider the detuning from the resonant frequency $\omega = 1/2$ to construct the solution in its neighbourhood. The detuning $\frac{1}{2}M\Delta$ is defined by

$$M\Delta = 2\omega - 1 \text{ or } \omega = \frac{1}{2}(1 + M\Delta). \tag{2.23}$$

Since the period of the piston input, $M\sin(2\pi\omega t)$, is $\frac{1}{\omega}$, we seek solutions such that $g(t + \frac{1}{\omega}; \tau) = g(t; \tau)$, then

$$g(t-2;\tau) = g\Big(t + \frac{1}{\omega} - 2; \tau\Big) = g\Big(t - \frac{2M\Delta}{1+M\Delta}; \tau\Big) \tag{2.24}$$

$$= g\Big(t - 2M\Delta + O(M^2); \tau\Big) \tag{2.25}$$

$$= g(t;\tau) - \frac{M\Delta}{\omega}\frac{\partial g}{\partial t} + O(M^2), \tag{2.26}$$

on noting (2.23). Then (2.19) becomes

$$M\frac{\partial g}{\partial \tau} + \frac{\gamma+1}{2}Mg\frac{\partial g}{\partial t} + \frac{M\Delta}{2\omega}\frac{\partial g}{\partial t} = \frac{1}{2}\sin(2\pi\omega t). \tag{2.27}$$

With the substitutions

$$\eta = \omega t,\ \overline{\tau} = \frac{\tau}{2\varepsilon} \text{ and } F = (\gamma+1)M\omega g + M\Delta,$$

(2.27) becomes

$$\frac{\partial F}{\partial \overline{\tau}} + F\frac{\partial F}{\partial \eta} = A\sin(2\pi\eta), \tag{2.28}$$

where $A = (\gamma+1)M\omega$ and $\int_0^1 F(s)\mathrm{d}s = M\Delta$, which agrees with [35] on allowing for the change of notation. The evolution of the motion is given by a simple wave equation with a periodic r.h.s.

The exact solution of (2.28) can be expressed in terms of elliptic functions; a detailed analysis is given in [11].

Figure 3, where the vertical axis is F and the horizontal axis is τ, shows the growth and distortion of the signal until a shock forms in cycle 8 of the piston. Figure 4 shows that for sufficiently large Δ outside the resonant band, a shock in cycle 41 dissipates to zero strength as the cycle number increases indefinitely, leaving a periodic linear solution. These figures are taken from [11].

3. Experiment 2: Variable tube cross-section, resonant macrosonic synthesis, closed cavities

The experiments described in Lawrenson *et al.* [22] involve resonant oscillations in closed cavities of variable cross-section, typically shaped like a cone, a horn-cone or a bulb. Figure 5 contrasts the output from a horn-cone with that of a straight cylinder. The latter output contains shocks and the amplitude is significantly less than that of the horn-cone, where the signal is continuous.

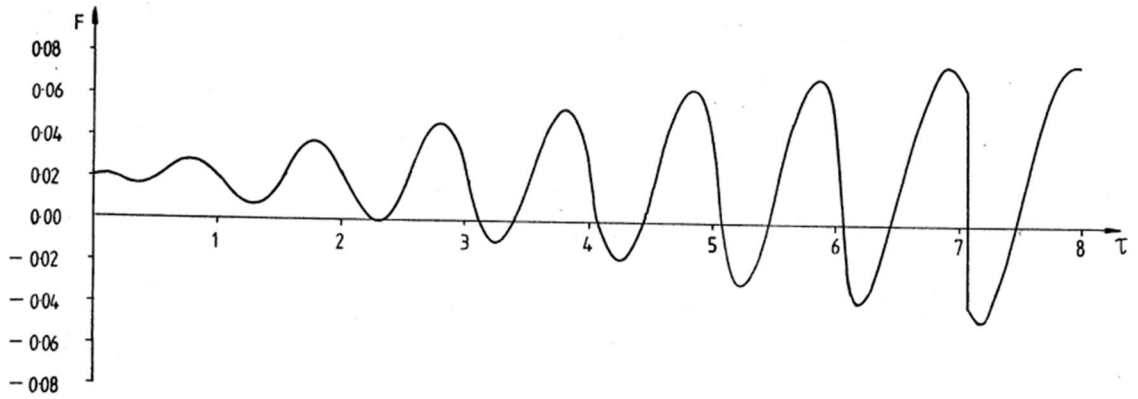


FIGURE 3. Evolution over 8 cycles; $A = 0.01$, $\Delta = 0.02$.

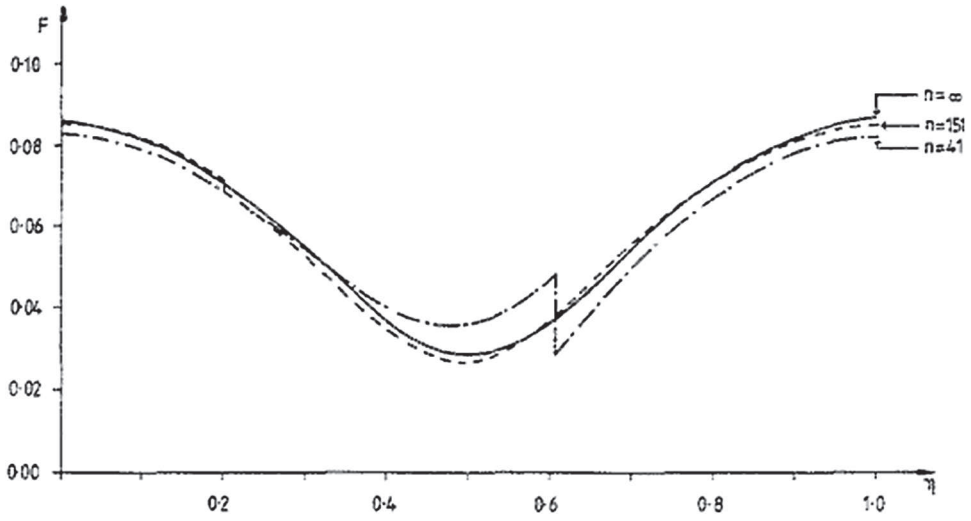


FIGURE 4. Outside resonant band. $A = 0.01$, $\Delta = 0.06$.

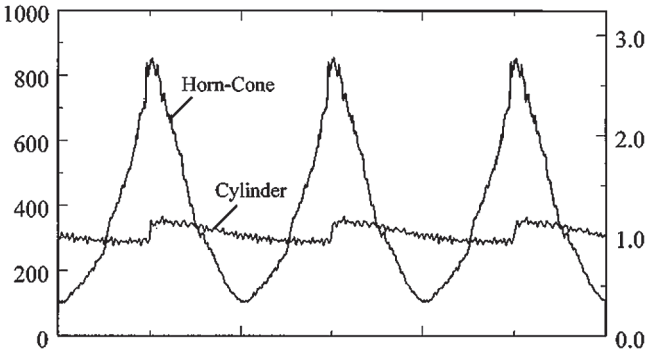


FIGURE 5. Output pressure from cylinder and horn-cone, from [22].

The essential experimental results are:

- For a straight closed tube, energy is lost through heat generated by shocks, thus limiting the resulting pressure amplitude.
- Shocks (acoustic saturation) can be avoided by shaping the resonator.
- With no shocks, the input energy can produce higher pressures with peak acoustic overpressure exceeding 340% of ambient pressure.
- Nonlinear effects in high-amplitude standing waves are strongly dependent on the shape of the resonator.

The analytical underpinning for these experimental results is given in Mortell and Seymour [26] for the periodic case, while a numerical solution is given in Ilinskii *et al.* [19], see also Chun and Kim [9]. The evolution of the motion is described in Mortell *et al.* [24].

While resonant oscillations in a straight closed tubes are well documented over many years, the question as to whether area variation can affect the output and prevent shocks is less well studied, with no definitive results produced until those of [26].

Mortell and Seymour [25] showed that small variations that satisfy the conditions of geometrical acoustics do not prevent shock formation. Further analytical studies were those of Keller [21], Ockendon *et al.* [30], Chester [8] and a numerical study of Hussain *et al.* [18]. The above analytic studies all began by an area variation that is a perturbation from the straight tube, which itself is a limiting case. The pioneering experiments of Lawrensen *et al.* [22] showed the effects of area variation, with no restriction on the magnitude of the variation, and the analytical work of Mortell and Seymour [26] to describe the experimental output followed. Figure 6 shows the hysteresis curves for a closed cone and a bulb, *i.e.*, the fundamental acoustic pressure as a function of frequency in the neighbourhood of resonance, and compares the experimental output in [22] with the analytical results in [26].

3.1. Nonlinear equations for variable tube area, $s(x)$

Using the same notation as in Section 2, the dimensionless equations of conservation of mass and momentum are:

$$\frac{\partial(s\rho)}{\partial t}+\frac{\partial}{\partial x}(su\rho)=0,\ \ \frac{\partial u}{\partial t}+u\frac{\partial u}{\partial x}+\rho^{\gamma-2}\frac{\partial \rho}{\partial x}=\mu\frac{\partial}{\partial x}(\frac{1}{s}\frac{\partial}{\partial x}(su))-a(t), \tag{3.1}$$

where $s(x)$ is the cross-sectional area and $a(t)$ is the acceleration applied along the axis of the tube that is closed at both ends. μ is a dimensionless damping coefficient that includes viscosity, and the condensation is $e(x,t)=\rho(x,t)-1$. For small $|e|$ the equation of state is

$$p=\rho^{\gamma}=1+\gamma e+\frac{\gamma(\gamma-1)}{2}e^2+\ldots,$$

and γ is the adiabatic constant.

A new variables $f(x,t)$ is introduced by

$$f(x,t)=s(x)u(x,t). \tag{3.2}$$

Since the resonator is closed at both ends, the boundary conditions are

$$f(0,t)=0=\ f(1,t). \tag{3.3}$$

and the applied acceleration is specified as

$$a(t)=\varepsilon^3\cos\theta. \tag{3.4}$$

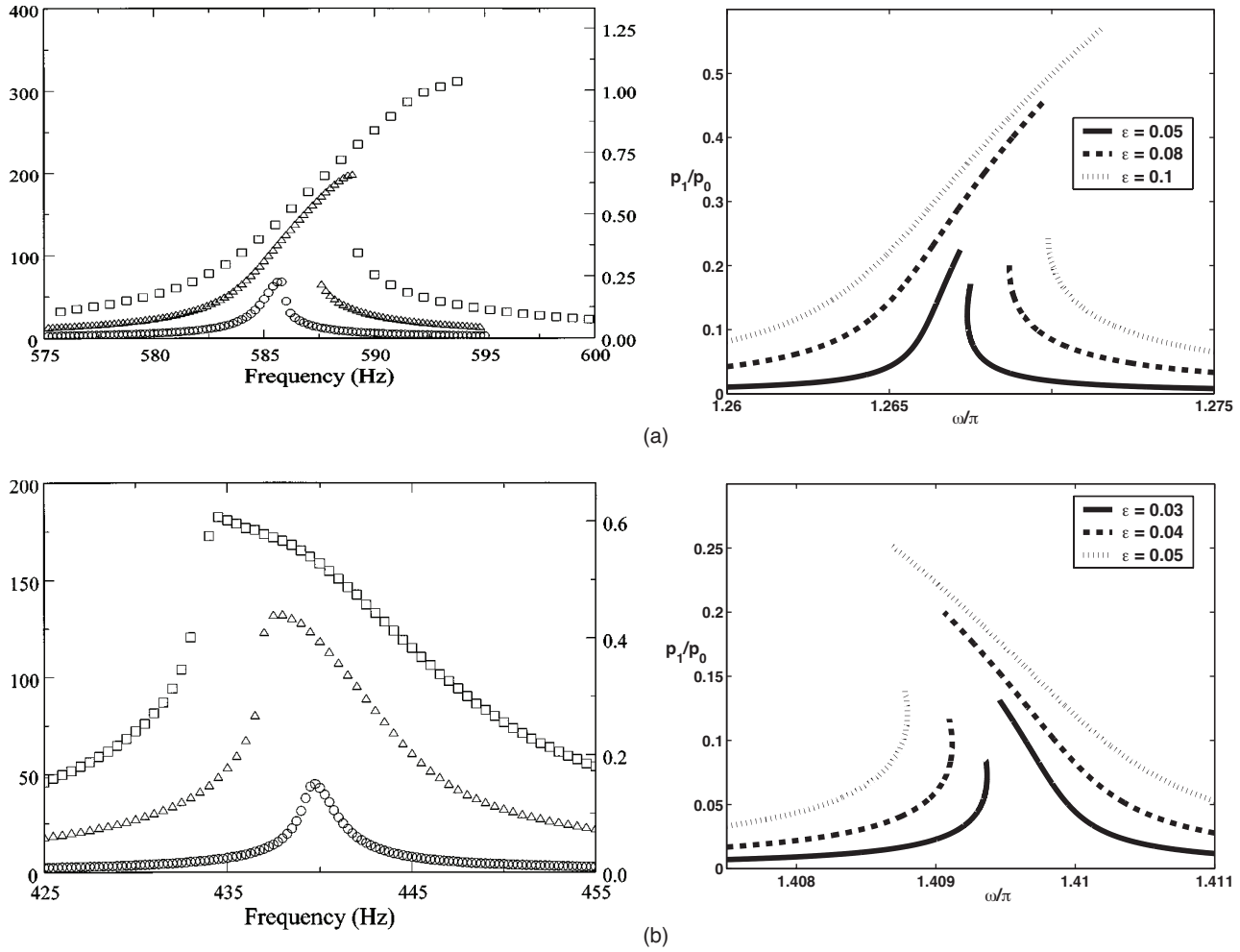


FIGURE 6. *Left*, Lawrenson experiment from [22]; *right*, theoretical from [26]. (a) Cone response; (b) bulb response.

where $\theta = \omega t$, and $0 < \varepsilon^3 \ll 1$ is the magnitude of the applied acceleration. We seek the evolution of small amplitude solutions that in the steady periodic state have the same period as the external forcing:

$$f\left(x, t + \frac{2\pi}{\omega}\right) = f(x,t) = O(\varepsilon). \tag{3.5}$$

It should be noted that, with an input at $O(\varepsilon^3)$, an output at $O(\varepsilon)$ is assumed.

3.2. Multiscale expansion for the evolution of continuous solutions

We seek solutions with period 2π in θ and assume a perturbation expansion of the form:

$$\begin{aligned} e(x,\theta) &= \varepsilon e_1(x,t;\tau) + \varepsilon^2 e_2(x,t;\tau) + \varepsilon^3 e_3(x,t;\tau) + \dots, \\ f(x,\theta) &= \varepsilon f_1(x,t;\tau) + \varepsilon^2 f_2(x,t;\tau) + \varepsilon^3 f_3(x,t;\tau) + \dots, \\ \omega &= \omega(\varepsilon) = \lambda_1 + \varepsilon^2 \delta + \dots \end{aligned} \tag{3.6}$$

and $\mu = \varepsilon^2\mu_1$, where $|e_i|, |f_i| = O(1)$, $i = 1, 2, 3\ldots$ Also we define $\tau = \varepsilon^2 t$, the slow time over which the forcing, the detuning $\varepsilon^2\delta$, the damping $\varepsilon^2\mu_1$ and the nonlinearity balance. λ_1 is the fundamental eigenvalue or resonant frequency. Substituting the expansion (3.6) into equations (3.1) yields the Webster horn equation at $O(\varepsilon)$

$$\lambda_1^2 \frac{\partial^2 f_1}{\partial\theta^2} - s(x)\frac{\partial}{\partial x}\left(\frac{1}{s(x)}\frac{\partial f_1}{\partial x}\right) = 0, \tag{3.7}$$

with the boundary conditions

$$f_1(0, t; \tau) = 0, \;\; f_1(1, t; \tau) = 0. \tag{3.8}$$

We note that due to (3.8), the solution for f_1 is a standing wave. By choosing

$$f_1(x, \theta; \tau) = A(\tau)\phi(x)\sin[\theta + \nu(\tau)], \tag{3.9}$$

where $A(\tau)$ is an amplitude and $\nu(\tau)$ a phase, the eigenfunction $\phi(x)$ satisfies

$$\frac{\mathrm{d}}{\mathrm{d}x}\left(\frac{1}{s(x)}\frac{\mathrm{d}\phi}{\mathrm{d}x}\right) + \frac{\lambda_1^2}{s(x)}\phi = 0, \;\; \phi(0) = 0, \;\; \phi(1) = 0, \tag{3.10}$$

and is normalized by $\int_0^1 s^{-1}(x)\phi^2(x)\mathrm{d}x = 1$. The area variation $s(x)$ must be such that there is an infinity of discrete eigenvalues λ_n such that $\lambda_n \neq n\lambda_1$, $n = 2, 3, \ldots$, *i.e.* the eigenvalues are incommensurate; this is essential for the theory. It is also essential for the theory that the spectrum is sufficiently incommensurate *i.e.*, that $|\lambda_2 - 2\lambda_1|$ is sufficiently large. This is discussed in detail in [2] in the context of the number of modes required for an accurate approximation. The condensation is given by

$$e_1(x, \theta; \tau) = \frac{A(\tau)}{\lambda_1 s(x)}\phi'(x)\cos[\theta + \nu(\tau)]. \tag{3.11}$$

In a similar way at $O(\varepsilon^2)$

$$f_2(x, \theta; \tau) = A^2(\tau)B(x)\sin 2[\theta + \nu(\tau)], \tag{3.12}$$

where

$$\frac{\mathrm{d}}{\mathrm{d}x}\left(\frac{1}{s}\frac{\partial B}{\partial x}\right) + \frac{(2\lambda_1)^2}{s}B = C_2(x), \;\; B(0) = 0, \;\; B(1) = 0, \tag{3.13}$$

and $C_2(x)$ is a function of $\phi(x)$ and $\phi'(x)$. Since $2\lambda_1$ is not an eigenvalue there is no restriction on $A(\tau)$ required to ensure a solution of (3.13).

At $O(\varepsilon^3)$ we seek a solution of the form

$$f_3(x, \theta; \tau) = P(x, \tau)\sin[\theta + \nu(\tau)] + Q(x, \tau)\cos[\theta + \nu(\tau)] + \text{terms in } 3\theta. \tag{3.14}$$

As in (3.13), the equation for terms in 3θ involves $(3\lambda_1)^2$, but as $3\lambda_1$ is not an eigenvalue there is no required restriction on $A(\tau)$.

The equations for $P(x, \tau)$ and $Q(x, \tau)$ involve the eigenvalue λ_1 and have zero boundary conditions. There are now restrictions on $A(\tau)$ and $\nu(\tau)$ to ensure a solution, and the Fredholm alternative gives

$$NA^3\cos\nu(\tau) - M = 2\delta\lambda_1 A\cos\nu + 2\lambda_1^2[A'\sin\nu + A\nu'\cos\nu] + \lambda_1^3\mu_1 A\sin\nu, \tag{3.15}$$

and

$$NA^3 \sin\nu(\tau) = 2\delta\lambda_1 A \sin\nu - 2\lambda_1^2[A'\cos\nu - A\nu'\sin\nu] - \lambda_1^3\mu_1 A\cos\nu,$$

where the coefficients M and N, which depend on the eigenfunction $\phi(x)$, are constants involving integrals over a period of lower order solutions, and are the same as in the periodic problem, see equation (40) in [26]. Now (3.15) and (3.16) may be put in the form

$$2\lambda_1^2 A' = -M\sin\nu - \lambda_1^3\mu_1 A, \tag{3.16}$$

and

$$2\lambda_1^2 A\nu' = NA^3 - M\cos\nu - 2\lambda_1\delta A. \tag{3.17}$$

In the steady periodic state, as $\tau\to\infty$, the amplitude $A(\infty)$, with $A'=0$, $\nu'=0$, is determined by

$$NA^3 - [M^2 - (\lambda_1^3\mu_1 A)^2]^{1/2} - 2\lambda_1\delta A = 0, \tag{3.18}$$

and $\nu(\infty)$ is given by (3.16) with $A'=0$. When there is no damping, $\mu_1=0$, the steady state is

$$NA^3 - 2\delta\lambda_1 A = M, \tag{3.19}$$

which agrees with the result in [26]. Equation (3.19) is the *amplitude-frequency relation* and produces hysteresis curves, see Figure 6. $N>0$ for a cone or horn-cone and $N<0$ for a bulb, giving a hardening or softening response, respectively. The details can be found in [24] or [26].

The simplest example is that of a cone resonator with $s(x)=(1+kx)^2$ for some constant k. To find the eigenvalues and corresponding eigenfunctions for cone and bulb shapes, exact solutions to (3.7) are constructed using the methods described in Varley and Seymour [38]. The form of the eigenfunction for the cone is $\phi(x) = (1+kx)F' - kF$, where $F(x)$ satisfies $F''+\lambda^2 F=0$. Then direct substitution confirms that $\phi(x)$ satisfies (3.7) and the conditions $\phi(0)=\phi(1)=0$ yield the eigenvalue equation

$$\tan\lambda = \frac{\lambda k^2}{k^2+\lambda^2[1+k]}. \tag{3.20}$$

In the experiments of Lawrenson *et al.* [22]) $k=7$, when (3.20) gives $\lambda_1 = 1.27\pi$, $\lambda_2 = 2.21\pi$ and $\lambda_3 = 3.17\pi$, which are clearly incommensurate. Figure 7, taken from [24], is the phase plane for a parameter set corresponding to a cone ($\delta=0.5$, $M=0.3282$, $N=16.688$, $\lambda_1=1.27\pi$ and $\mu_1=0$). Since $N>0$ the amplitude-frequency curve bends to the right, *i.e.*, a hardening of the system. Points on the curve (3.18) correspond to fixed points of A for the nonlinear coupled equations (3.16), (3.17). For $A>0$ there is a stable spiral close to $A=0$, $\nu=0$ with clockwise sense, and a saddle point with an anticlockwise stable spiral near $A=0.5$, $\nu=0$.

A comparison of the input acceleration (3.4) at $O(\varepsilon^3)$ with the assumed output (3.6) at $O(\varepsilon)$, with the boundary conditions (3.3), shows that the basic assumption used here is that the flow can be constructed as an iteration about a linear standing wave. Equations (3.9) and (3.10) show f_1 is a linear standing wave with a slowly modulated amplitude $A(\tau)$ and phase $\nu(\tau)$, which are both determined at $O(\varepsilon^3)$ by (3.16) and (3.17).

In the case of varying area the solution is found as the sum of modes where, for a closed tube, the dominant first harmonic approximation is sufficient. However, the expansion must be taken to $O(\varepsilon^3)$ as compared with $O(\varepsilon^2)$ for a straight tube. A consequence of this is the presence of interaction terms so that the nonlinearization technique, which relies on simple wave solutions, cannot be applied. Such interaction terms arise in the case of resonance in a straight open tube, see Seymour and Mortell [34], Chester [7], Cox and Kluwick [14], Mortell and

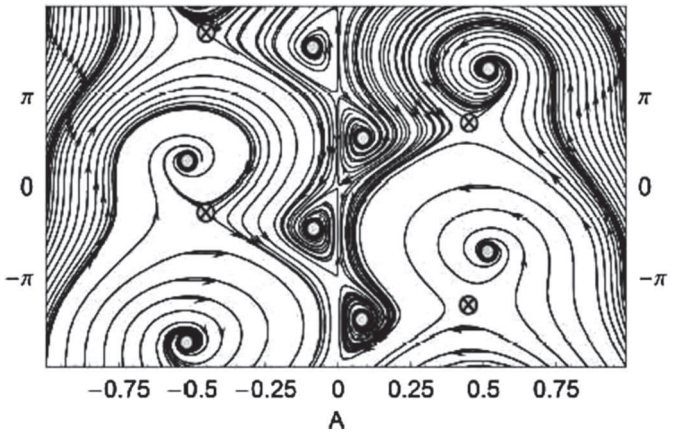


FIGURE 7. Phase plot for cone, $\delta = 0.5$.

Seymour [28]. The interaction term involves the integral $\int g^2(t)\mathrm{d}t$ over a period. Resonance in open axisymmetric tubes is dealt with in Amundsen *et al.* [2] using a modal approach.

4. Experiment 3: Resonant sloshing of shallow water in a tank

The basic experiment is described in Chester and Bones [6]. This brings into play the effect of frequency dispersion on an otherwise hydraulic flow. The latter is mathematically equivalent to the motion of a polytropic gas with constant $\gamma = 2$. For an analysis of this case see [29], or Section 2.2 here.

Water is contained in a tank where the depth of water H is small compared with the length of the tank L, *i.e.*, $\delta = H/L \ll 1$. The amplitude l of the wavemaker is also small compared with L, so $\varepsilon = l/L \ll 1$. The behaviour of the fluid is then characterized by the two (independent) small parameters δ and ε. In the experiment described in [6], $L = 24$, $H = 0.5, 1, 2$, $l = 0.031, 0.062, 0.124$, with the width of the tank 6 and the height 8, all measured in inches.

The experimental results in [6] show.

- The number of oscillations in the waveform decreases by one until just above the resonant frequency there is a solitary and well-defined peak in each cycle.
- At certain discrete frequencies abrupt changes in the amplitude occur.
- Within a defined frequency band about the resonant frequency the amplitude of the response is significantly larger than that of the wave-maker.
- At both ends of the spectrum about resonance the waveform approximates to the sinusoidal form expected from linear theory.

The theory underlying these experiments was given by Chester [5] for the periodic motion, Cox and Mortell [12] for the evolution to the periodic state, and by Ockendon and Ockendon [29] describing asymptotic results for the periodic motion, see also Amundsen *et al.* [1]. Here, we follow the approach in [12].

4.1. Dimensionless equations

Dimensionless variables are introduced by

$$\varphi' = \frac{\varphi}{Lc_0}, \qquad x' = \frac{x}{L}, \qquad \omega' = \frac{\omega L}{2\pi c_0}, \qquad u' = \frac{u}{c_0},$$
$$t' = \frac{\omega}{\pi}t, \qquad z' = \frac{z}{H}, \qquad \eta' = \frac{\eta}{H} \quad \text{and} \quad p' = \frac{p_0}{\rho_0 c_0^2},$$

where $\varphi = \frac{\partial \varphi}{\partial x}$ is the velocity potential, p_0 is the pressure on the free surface, ω is the frequency of the wave maker and $c_0 = (gH)^{\frac{1}{2}}$ is the long-wave speed. Dropping all primes, the velocity potential satisfies

$$\delta^2 \frac{\partial^2 \varphi}{\partial x^2} + \frac{\partial^2 \varphi}{\partial z^2} = 0, \qquad 0 < x < x_w = 1 - \varepsilon \cos(\pi t), \quad -1 < z < \eta(x,t), \tag{4.1}$$

subject to the boundary conditions on the free surface $z = \eta(x,t)$, and the bottom and ends of the tank. The boundary condition at the wave maker, which imparts a small amplitude velocity at $x_w = 1 - \varepsilon \cos(\pi t)$, is

$$u(x_w, z, t) = \frac{\partial \varphi}{\partial x}(x_w, z, t) = 2\pi\varepsilon\omega \sin(\pi t), \qquad -1 < z < \eta(x,t). \tag{4.2}$$

The tank is closed at $x = 0$:

$$\frac{\partial \varphi}{\partial x}(0, z, t) = 0, \qquad -1 < z < \eta(x,t), \tag{4.3}$$

while the bottom is impermeable so that

$$\frac{\partial \varphi}{\partial z}(x, -1, t) = 0 \qquad \text{on } z = -1. \tag{4.4}$$

On the free surface the dynamic and kinematic conditions imply

$$2\omega \frac{\partial \varphi}{\partial t} + \frac{1}{2}\left[\left(\frac{\partial \varphi}{\partial x}\right)^2 + \delta^{-2}\left(\frac{\partial \varphi}{\partial z}\right)^2\right] + \eta = 0 \tag{4.5}$$

and

$$\frac{\partial \varphi}{\partial z} - \delta^2 \left[2\omega \frac{\partial \eta}{\partial t} + \frac{\partial \eta}{\partial x}\frac{\partial \varphi}{\partial x}\right] = 0. \tag{4.6}$$

The nonlinearity enters through (4.5) and (4.6).

4.2. Perturbation expansion

We assume an expansion for the velocity potential φ and free surface elevation η of the form

$$\begin{aligned} \varphi(x, z, t; \varepsilon) &= \varepsilon \varphi_0(x, z, t) + \varepsilon^{3/2} \varphi_1(x, z, t) + O(\varepsilon^2), \\ \eta(x, t; \varepsilon) &= \varepsilon \eta_0(x, t) + \varepsilon^{3/2} \eta_1(x, t) + O(\varepsilon^2). \end{aligned} \tag{4.7}$$

For a balance between nonlinearity and frequency dispersion, following [5] and [29], the relationship between the independent parameters δ and ε is chosen to be

$$\delta^2 = \kappa \varepsilon^{1/2}, \tag{4.8}$$

where it is assumed at this stage that the amplitude of the periodic flow is $O(\varepsilon^{1/2})$ at resonance. The period of the input in (4.2) is 2, which gives a dimensionless frequency of 1/2, and, since the length of the tank and wave speed are both normalized to unity, the round-trip travel time in the tank is also 2. So, the period of the input equals the travel time at the frequency 1/2, and thus the fundamental resonance is $\omega = 1/2$. In dimensional

variables $\frac{2\pi}{\omega} = \frac{2L}{c_0}$ at resonance, giving $\omega = 1/2$ in dimensionless variables. The detuning parameter $\overline{\Delta}$ is given by

$$2\omega = 1 + \varepsilon^{1/2}\overline{\Delta}. \tag{4.9}$$

The expansions (4.7) are used to first find the periodic solution, and then an adjustment is made to follow the evolution by introducing a slow time variable $\tau = \varepsilon t$. Using (4.7) and (4.8) in (4.1) and (4.3) yields

$$\varphi_0(x,z,t) = \theta_0(x,t),\ \varphi_1(x,z,t) = \theta_1(x,t) - \frac{1}{2}\kappa(1+z)^2\frac{\partial^2\theta_0}{\partial x^2}, \tag{4.10}$$

and then the free surface conditions, with (4.9), imply

$$\frac{\partial^2\theta_0}{\partial x^2} - \frac{\partial^2\theta_0}{\partial t^2} = 0, \tag{4.11}$$

$$\frac{\partial^2\theta_1}{\partial x^2} - \frac{\partial^2\theta_1}{\partial t^2} = \kappa\left(\frac{1}{6}\frac{\partial^4\theta_0}{\partial x^4} - \frac{1}{2}\frac{\partial^4\theta_0}{\partial x^2\partial t^2}\right) + 2\overline{\Delta}\frac{\partial^2\theta_0}{\partial x^2}. \tag{4.12}$$

The dispersion terms involving κ and the detuning term $\overline{\Delta}$ appear in (4.12), but the nonlinearity will not appear until $O(\varepsilon^2)$. Now

$$\theta_0(x,t) = g(\alpha) + f(\beta),\ \alpha = t - x,\ \beta = t + x - 1, \tag{4.13}$$

and on substituting into (4.12) gives

$$\frac{\partial\theta_1}{\partial x} = \frac{1}{12}\kappa\left[g'''(\alpha) - f'''(\beta)\right] - \frac{1}{6}\kappa x\left[g^{iv}(\alpha) + f^{iv}(\beta)\right] - \frac{1}{2}\overline{\Delta}\left[g'(\alpha) - f'(\beta)\right] + \overline{\Delta}x\left[g''(\alpha) + f''(\beta)\right]. \tag{4.14}$$

With $u = \varepsilon\frac{\partial\varphi_0}{\partial x} + \ldots = \varepsilon\left[f'(\beta) - g'(\alpha)\right] + \ldots$ the boundary conditions at $x = 0$ and at $x = 1$, with $\frac{\partial\varphi_0}{\partial x}(1,t) = \pi\sin(\pi t)$, imply the linear difference equation for h at resonance, $\omega = 1/2$,

$$\pi\sin(\pi t) = h(t) - h(t-2),$$

where $h(t) = f'(t)$. The linear solution then is

$$\varepsilon h(t) = \frac{1}{2}\pi t\varepsilon\sin\pi t, \tag{4.15}$$

which shows the initial amplitude growth at resonance.

If we use the approximation $u = \varepsilon\frac{\partial\varphi_0}{\partial x} + \varepsilon^{3/2}\frac{\partial\varphi_1}{\partial x}$ the boundary conditions at $x = 0$ and at $x = 1$, where $\frac{\partial\varphi_1}{\partial x}(1,t) = \overline{\Delta}\pi\sin(\pi t)$, yield the linear differential-difference equation for h :

$$2\pi\varepsilon\omega\sin(\pi t) = \varepsilon[h(t) - h(t-2)] + \varepsilon^{3/2}[-\frac{1}{3}\kappa h'''(t) + 2\overline{\Delta}h'(t)], \tag{4.16}$$

where frequency dispersion and detuning are included and the periodicity condition $h(t) = h(t-2)$ is used, and

$$u(x,t) = \varepsilon[h(t+x-1) - h(t-x-1)].$$

The nonlinear terms come from the free surface condition and can be included in (4.16) after a long calculation at $O(\varepsilon^2)$, see [12] or [29]. However, such a calculation can be avoided by nonlinearization as in Section 2.2, see also [27] and [28].

We note that the linear travel time in (4.16) is 2, while the nonlinear travel time is

$$2+(\gamma+1)\varepsilon h(t), \text{ with } \gamma=2, \tag{4.17}$$

see (2.17). This comes from the observation that the equations for the underlying hydraulic flow correspond to those of a polytropic gas with $\gamma=2$. Then, on inserting the nonlinear travel time, (4.16) becomes

$$\pi\omega\sin(\pi t)=\frac{3}{2}\varepsilon h(t)h'(t)+\varepsilon^{1/2}[-\frac{1}{6}\kappa h'''(t)+\overline{\Delta}h'(t)]. \tag{4.18}$$

With $R(t)=\varepsilon^{1/2}h(t)$, (4.18) becomes

$$\pi\omega\sin(\pi t)=\frac{3}{2}R(t)R'(t)+\overline{\Delta}R'(t)-\frac{1}{6}\kappa R'''(t), \tag{4.19}$$

and this is a periodically forced, steady state KdV equation as in [12] and [29]. At resonance, $\omega=1/2$, with $\overline{\Delta}=\kappa=0$, the solution (2.21) is recovered from (4.19) on noting $\frac{\gamma+1}{2}=\frac{3}{2}$.

4.3. Multiscale expansion for evolution

We show how the differential-difference equation (4.16) can be transformed into a nonlinear p.d.e. by using nonlinearization and a two-variable expansion technique. The time scale identified by t is a measure of time for a signal to travel the length of the tank, while $\tau=\varepsilon t$ measures time over which nonlinear effects become significant, and $\tau\ll t$ is required. We assume an expansion of the form

$$h(t;\varepsilon)=h_0(t,\tau)+\varepsilon h_1(t,\tau)+\dots, \tag{4.20}$$

and note, as in (2.8)

$$h(t-2;\varepsilon)=h_0(t-2;\tau)-2\varepsilon\frac{\partial h_0}{\partial\tau}(t-2;\tau)+\varepsilon h_1(t-2;\tau)+\dots \tag{4.21}$$

We seek solutions such that

$$h_i(t-2;\varepsilon)=h_i(t;\tau),\ i=0,1,2\dots \tag{4.22}$$

i.e., they are periodic in t with the period of the input and slowly modulated on the time scale τ. Then (4.16) reduces to, with terms at $O(\varepsilon^{3/2})$ neglected,

$$\varepsilon\frac{\partial h_0}{\partial\tau}+\varepsilon\frac{3}{2}h_0\frac{\partial h_0}{\partial t}+\varepsilon^{1/2}\overline{\Delta}\frac{\partial h_0}{\partial t}-\frac{\delta^2}{6}\frac{\partial^3 h_0}{\partial t^3}=\pi\omega\sin(\pi t), \tag{4.23}$$

on using (4.21), (4.22), nonlinearization and $\delta^2=\kappa\varepsilon^{1/2}$. The appropriate initial condition is $h_0(t;0)=0$, which corresponds to a fluid at rest. On noting (4.22), integration of (4.23) over one period in t yields the mean condition

$$\int_0^2 h_0(t;\tau)\mathrm{d}t=0, \tag{4.24}$$

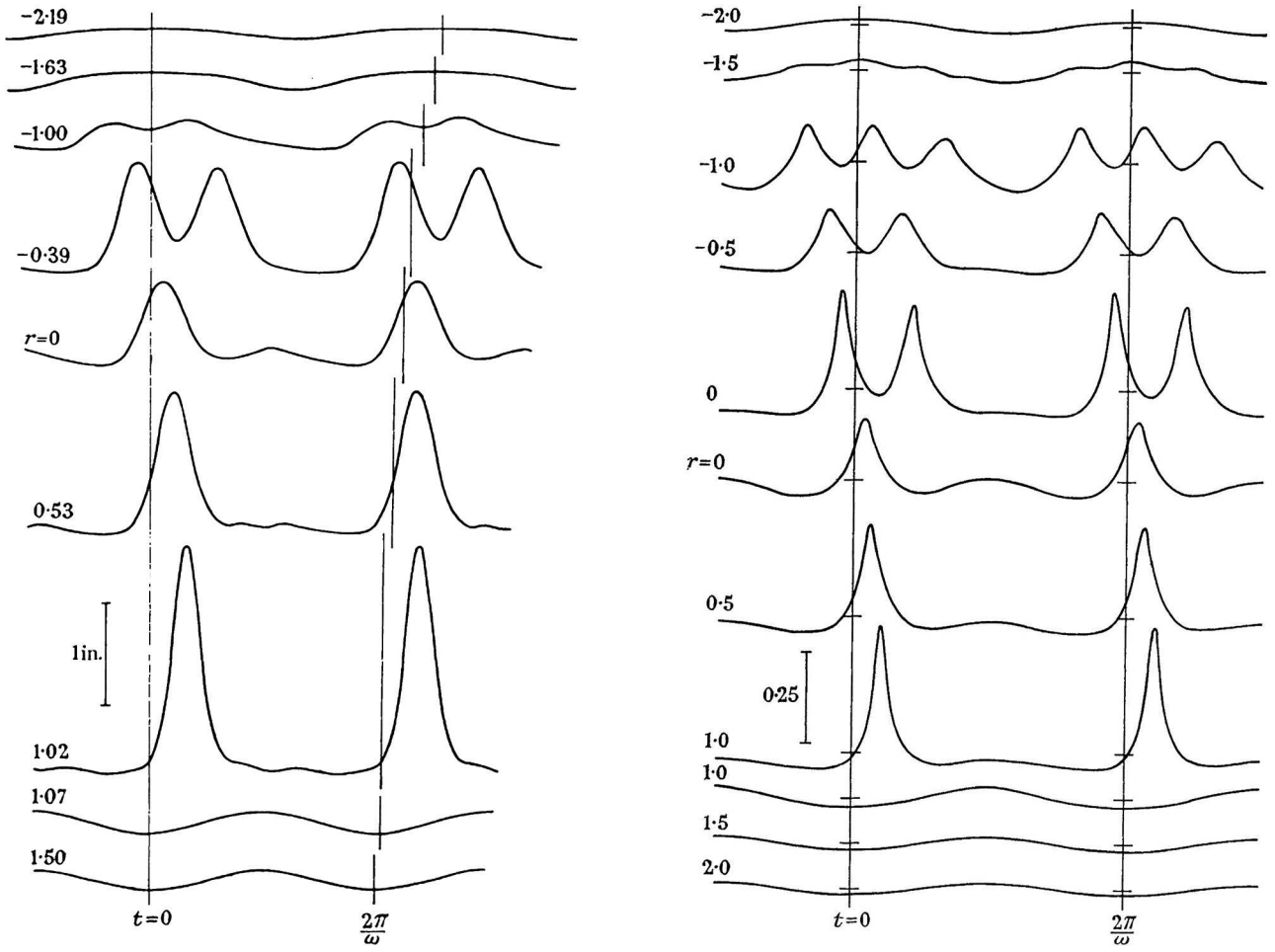


FIGURE 8. Experimental (*left*) and theoretical results (*right*) from [6] and [5].

and this refers to $h_0(t;\tau)$ on lines of constant τ. The physical solution requires that $h_0(t;\tau)$ be evaluated along $\tau = \varepsilon t$, $t \geqslant 0$.

The term $\varepsilon \frac{\partial h_0}{\partial \tau}$ in (4.23) gives the initial growth of the signal, see equation (2.9), and the remaining terms give the periodic equation (4.19), so that (4.23) is uniformly valid.

From the definition of Δ and $\overline{\Delta}$ in (2.23) and (4.9), respectively, the detuning term in (4.23) can be written as $M\Delta \frac{\partial h_0}{\partial t}$ and then (2.27) and (4.23) coincide when $\delta = 0$ (no dispersion) and $\gamma = 2$.

Equation (4.23) is a *periodically forced KdV equation* subject to the periodicity condition (4.22) and represents the evolution of the signal h_0 on the boundary $x = 1$. The speed of the wave in the tank is unity and the velocity is determined by the linear superposition

$$\frac{\partial \theta_0}{\partial x} = [h_0(t + x - 1, \tau) - h_0(t - x - 1, \tau)].$$

The signal carried by the wave is given by the nonlinear p.d.e. (4.23), the periodicity condition (4.22) and the initial condition $h_0(t;0) = 0$.

Figure 8 shows the experimental output as the applied frequency moves through the resonant band as in [6] and the corresponding theoretical results given in [5]. It illustrates how as the frequency is reduced the

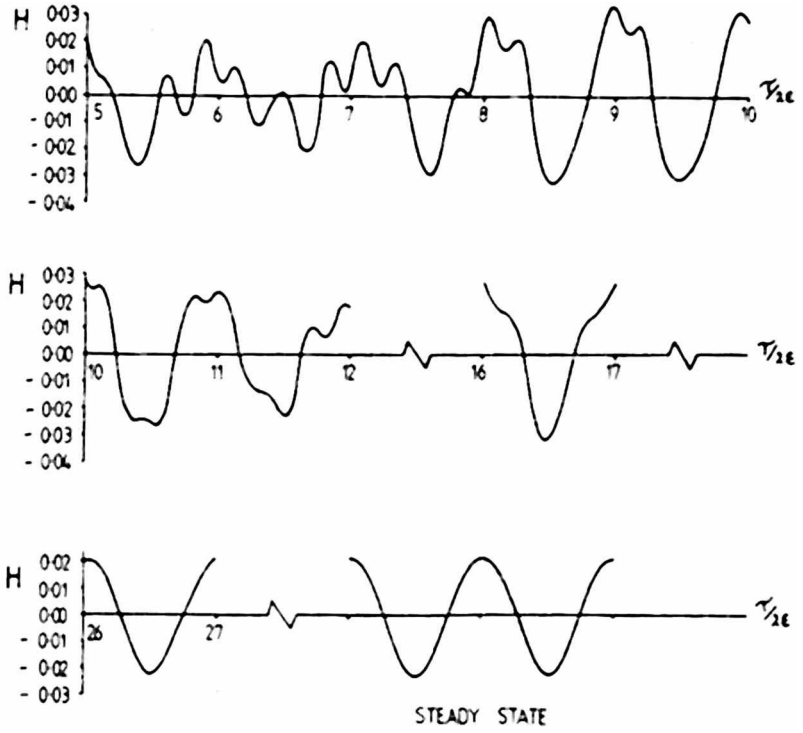


FIGURE 9. Evolution outside resonant band.

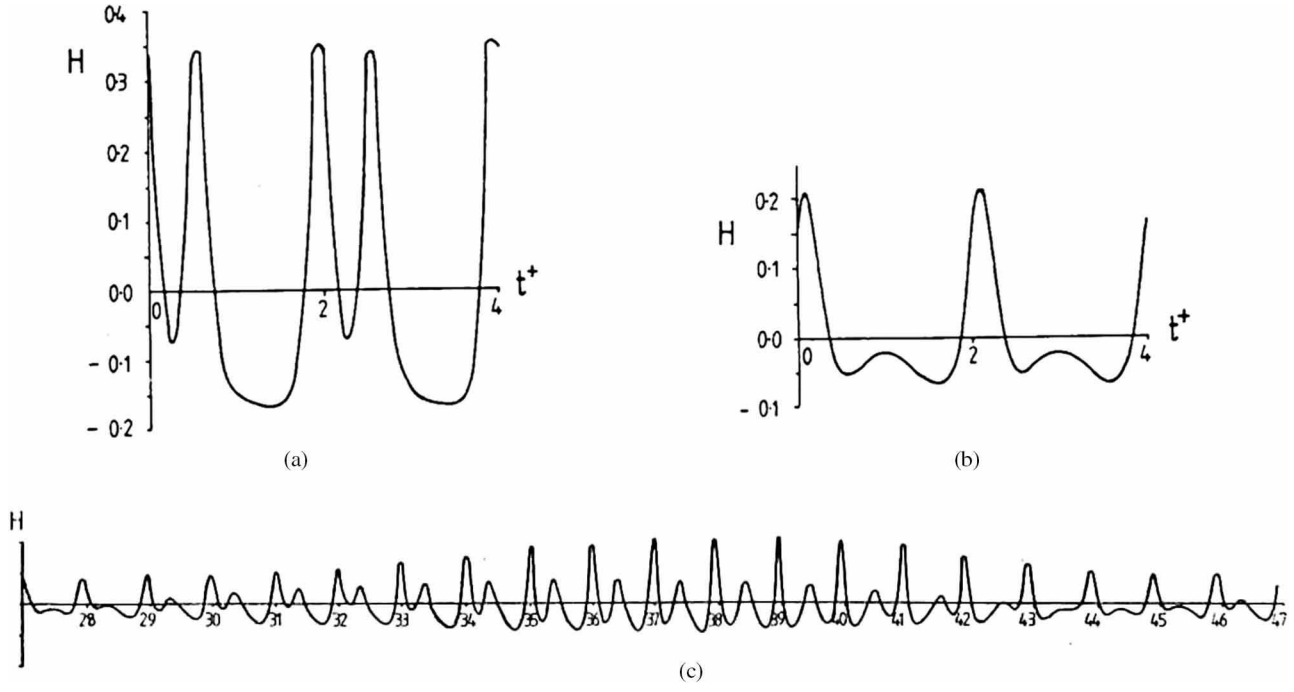


FIGURE 10. (a) and (b) Two solutions at a particular frequency. (c) Beat oscillations.

theoretical linear solution initially develops multiple peaks that reduce to a solitary peak just above resonance, as required by experiment.

Figure 9 shows the evolution of a signal that includes damping for a frequency outside the resonant band, culminating in a linear approximation steady state as in [12].

Figure 10c shows a "beat" oscillation that has a period 18 times larger than the period of the forcing term as calculated in [12]. Such beat solutions were observed experimentally in [6]. Figure 10a and b (taken from [12]) shows two solutions at a particular frequency; this non-uniqueness is the effect of hysteresis. The theoretical solutions in Figure 10a and c require an evolution equation to produce them numerically.

5. Conclusions and summary

Three experiments form the basis of the paper. It is shown how close attention to the experimental outputs points the way to an analytical model. Multiscale expansions explain the evolution to resonance.

The first experiment is classical acoustic resonance in a straight closed tube. The experiments described in [32] and the resultant outputs show that a theory involving linear superposition of nonlinear waves, as in (2.22), with the occurrence of shocks, as in (2.21), is required. The evolution equation (2.19) shows how the motion evolves from an initial flow at $O(M)$ to a final periodic flow at $O(M^{1/2})$. The nonlinearity of the travel time, equation (2.17), shows that the singularity in the acoustic solution then disappears to yield equation (2.20) that in turn yields a shock on using the mean condition.

The effect of a variable tube area on resonant acoustic oscillations is examined in Section 3. The fundamental experiment described in [22] shows that the essential ingredient is incommensurability of the eigenvalues of the linear system, which is a direct contrast to those of a straight tube. The consequence is that it is possible to produce high pressures without inducing acoustic saturation. The hardening or softening response of the system, depending on the shape of the container (tube), was a signal as to the type of asymptotic expansion required to explain the experimental results, as in [26]. In this case, the multiscale expansion is taken to third order – $\cos^3\theta$ can be written in terms of θ and 3θ – and the Fredholm alternative gives the required solutions (3.16) and (3.17) for the evolution of the amplitude and phase of the standing wave (3.9) at the initial order, $O(\varepsilon)$. Since there are nonlinear interaction terms at third order, the nonlinearization technique cannot be used as it depends on simple wave solutions.

A multiscale expansion is again used in resonant sloshing of shallow water in a tank. It is clear from the experiments that the KdV equation is involved through the appearance of a solitary, well-defined peak at resonance. The abrupt frequency change indicates hysteresis and an amplitude-frequency curve. The assumed perturbation expansion begins with a linear acoustic approximation at first order, followed by the appearance of dispersion and detuning at the next order. Then nonlinearization (4.17) brings in the effect of nonlinear terms at the third order, without a lengthy calculation as in [12]. The introduction of a slow time scale $\tau = \varepsilon t$ and a multiscale expansion then gives the evolution equation (4.23), which predicts the beat solution in Figure 10 and the two solutions corresponding to hysteresis.

References

[1] D.E. Amundsen, E.A. Cox and M.P. Mortell, Asymptotic analysis of the steady solutions of the KdVB equation with application to resonant sloshing. *Z. Angew. Math. Phys.* **58** (2007) 1008–1034.
[2] D.E. Amundsen, M.P. Mortell and B.R. Seymour, Resonant oscillations in open axisymmetric tubes. *Z. Angew. Math. Phys.* **68** (2017) 139.
[3] R. Betchov, Nonlinear oscillations of a column of gas. *Phys. Fluids* **1** (1958) 205–212.
[4] W. Chester, Resonant oscillations in closed tubes. *J. Fluid Mech.* **18** (1964) 44–64.
[5] W. Chester, Resonant oscillations of water waves I. Theory. *Proc. R. Soc. Lond. Ser. A: Math. Phys. Sci.* **306** (1968) 5–22.
[6] W. Chester and J.A. Bones, Resonant oscillations of water waves II. Experiment. *Proc. R. Soc. Lond. Ser. A: Math. Phys. Sci.* **306** (1968) 23–39.
[7] W. Chester, Resonant oscillations of a gas in an open-ended tube. *Proc. R. Soc. Lond. Ser. A: Math. Phys. Sci.* **377** (1981) 449–467.
[8] W. Chester, Nonlinear resonant oscillations of a gas in a tube of varying cross-section. *Proc. R. Soc. Lond. Ser. A: Math. Phys. Sci.* **444** (1994) 591–604.

[9] Y.-D. Chun and Y.-H. Kim, Numerical analysis for nonlinear resonant oscillations of gas in axisymmetric closed tubes. *J. Acoust. Soc. Am.* **108** (2000) 2765–2774.
[10] B.T. Chu and S.J. Ying, Thermally driven nonlinear oscillations in a pipe with travelling shock waves. *Phys. Fluids* **6** (1963) 1625–1637.
[11] E.A. Cox and M.P. Mortell, The evolution of resonant oscillations in closed tubes. *Z. Angew. Math. Phys.* **34** (1983) 845–866.
[12] E.A. Cox and M.P. Mortell, The evolution of resonant water-wave oscillations. *J. Fluid Mech.* **162** (1986) 99–116.
[13] E.A. Cox and M.P. Mortell, The evolution of nonlinear resonant oscillations in closed tubes: solution of the standard mapping. *Chaos* **2** (1992) 201–214.
[14] E.A. Cox and A. Kluwick, Resonant gas oscillations exhibiting mixed nonlinearity. *J. Fluid Mech.* **318** (1996) 251–271.
[15] S.U. Galiev, M.A. Il'Gamov and A.V. Sadykov, Periodic shock waves in a gas. *Fluid Dyn.* **5** (1970) 223–230.
[16] A.P. Gorkov, Nonlinear acoustic oscillations of a column of gas in a closed tube. *Inzhenerno-Flzicheski Jurnal* **3** (1963) 246–250.
[17] A.I. Gulyayev and V.N. Kusnetsov, Gas oscillations of large amplitude in closed tubes. *Inzh. Jurnal* **3** (1963) 236–245.
[18] M.A. Hussain, M. Kawatzaski and T. Fujioka, Finite amplitude standing waves in closed ducts with cross sectional area change. *Wave Motion* **42** (2005) 226–237.
[19] Y.A. Ilinskii, B.Lipkens, T.S. Lucas, T.W. VanDoren and E.A. Zabolotskaya, Nonlinear standing waves in an acoustical resonator. *J. Acoust. Soc. Am.* **104** (1998) 2664–2674.
[20] M.A. Ilgamov, R.G. Zaripov, R.G. Galiullin and V.B. Repin, Nonlinear oscillations of a gas in a tube. *Appl. Mech. Rev.* **49** (1996) 137–154.
[21] J.J. Keller, Nonlinear acoustic resonances in shock tubes with varying cross-sectional area. *Z. Angew. Math. Phys.* **28** (1977) 107–122.
[22] C.C. Lawrenson, B. Lipkens, T.S. Lucas, D.K. Perkins and T.W. VanDoren, Measurements of macrosonic standing waves in oscillating closed cavities. *J. Acoust. Soc. Am.* **104** (1998) 623–636.
[23] E. Lettau, Messungen un Gasschwingungen grosser Amplitude in Rohrleitgunen. *Deut Kraftfahrforsch* **39** (1939) 1–17.
[24] M.P. Mortell, K.F. Mulchrone and B.R. Seymour, The evolution of macrosonic standing waves in a resonator. *Int. J. Eng. Sci.* **47** (2009) 1305–1314.
[25] M.P. Mortell and B.R. Seymour, Pulse propagation in a nonlinear viscoelastic rod of finite length. *SIAM J. Appl. Math.* **22** (1972) 209–224.
[26] M.P. Mortell and B.R. Seymour, Nonlinear resonant oscillations in closed tubes of variable cross-section. *J. Fluid Mech.* **519** (2004) 183–199.
[27] M.P. Mortell and B.R. Seymour, Nonlinearization and waves in bounded media: old wine in a new bottle. *J. Phys. Conf. Ser.* **811** (2017) 012006.
[28] M.P. Mortell and B.R. Seymour, Nonlinear Waves in Bounded Media: The Mathematics of Resonance. World Scientific Publishing, London (2017).
[29] J.R. Ockendon and H. Ockendon, Resonant surface waves. *J. Fluid Mech.* **59** (1973) 397–413.
[30] H. Ockendon, J.R. Ockendon, M.R. Peake and W. Chester, Geometrical effects in resonant gas oscillations. *J. Fluid Mech.* **257** (1993) 201–217.
[31] R. Riemann, Uber die Fortpflanzung ebener Luftwellen von endlicher Schwingungsweite, Vol. VIII. Gottingun Abhandlungen, (1858) 43.
[32] R.A. Saenger and G.E. Hudson, Periodic shock waves in resonating gas columns. *J. Acoust. Soc. Am.* **32** (1960) 961–970.
[33] B.R. Seymour and M.P. Mortell, Resonant acoustic oscillations with damping: small rate theory. *J. Fluid Mech.* **58** (1973a) 353–373.
[34] B.R. Seymour and M.P. Mortell, Nonlinear resonant oscillations in open tubes. *J. Fluid Mech.* **60** (1973b) 733–750.
[35] B.R. Seymour and M.P. Mortell, A finite-rate theory of resonance in a closed tube: discontinuous solutions of a functional equation. *J. Fluid Mech.* **99** (1980) 365–382.
[36] B.R. Seymour and M.P. Mortell, The evolution of a finite rate periodic oscillation. *Wave Motion* **7** (1985) 399–409.
[37] B. Sturtevant, Nonlinear gas oscillations in pipes. Part 2. Experiment. *J. Fluid Mech.* **63** (1974) 97–120.
[38] E. Varley and B.R. Seymour, A method for obtaining exact solutions to partial differential equations with variable coefficients. *Stud. Appl. Math.* **78** (1988) 183–225.
[39] J.H.G. Verhagen and L. van Wijngaarrden, Nonlinear oscillations of fluid in a container. *J. Fluid Mech.* **22** (1965) 737–751.
[40] G.B. Whitham, Linear and Nonlinear Waves. John Wiley & Sons, New York (1974).

Copyright of Mathematical Modelling of Natural Phenomena is the property of EDP Sciences and its content may not be copied or emailed to multiple sites or posted to a listserv without the copyright holder's express written permission. However, users may print, download, or email articles for individual use.